Eur. Phys. J. B **37**, 213–221 (2004)
DOI: 10.1140/epjb/e2004-00049-5

THE EUROPEAN PHYSICAL JOURNAL B

Bound states of breathers in the Frenkel-Kontorova model

M. Meister[a] and L.M. Floría

Dpto. Física de la Materia Condensada, Facultad de Ciencias, and Instituto de Biocomputación y Física de Sistemas Complejos, Universidad de Zaragoza, 50009 Zaragoza, Spain

Received 6 November 2003 / Received in final form 18 December 2003
Published online 15 March 2004 –

Abstract. In the dissipative, driven standard Frenkel-Kontorova model propagating breathers exist as attractors of the dynamics. In collisions, these excitations interact through the phonons they emit. A possible result of a two-breather collision is a bound state of two breathers. After looking at phonons and breather collisions, we present phenomenological results on breather bound states obtained from lattice dynamics simulations. In particular, we find that bound states can be characterised by the distance between the two breathers they comprise and their propagation velocity. Contrary to the single breather case, several values of the propagation velocity are easily accessible to bound states at fixed model parameters. The results are interpreted on the basis of the observed phonon spectra. The latter can easily be explained as Doppler-shifted combination frequencies of breather harmonics and a discreteness-induced perturbation frequency.

PACS. 63.20.Ry Anharmonic lattice modes – 63.20.Pw Localized modes

1 Introduction

In the second half of the past century the important role that nonlinear excitations play in many areas of physics became clear beyond any reasonable doubt. Solitons and solitary waves, in particular kinks of nonlinear Klein-Gordon models, received most attention. The largest part of the investigations on nonlinear excitations was done for continua in the language of partial differential equations, though nonlinear lattices received attention, too. For an overview see [1, 2]. Within the context of nonlinear lattices, a new type of nonlinear excitation, or specific type of solitary wave, depending on the nomenclature one adheres to, became prominent: the intrinsically localised mode or discrete breather (DB). The latter expression refers to the similarity between these nonlinear excitations of discrete systems and breather solutions of partial differential equations (in particular sine-Gordon), which are solutions to the nonlinear equations of motion with an internal oscillation of some frequency ω_b.

The most basic example of a discrete breather is a nonlinear excitation which is localised at a fixed position in the system. Its dynamics is governed by the time evolution of the internal degree of freedom, which can be of oscillatory or rotational nature. After the first predictions [3–5] of intrinsically localised modes, these excitations quickly attracted much interest. There exist proofs of existence of breathers in both Hamiltonian [6, 7] and dissipative [8] systems. Stability [7, 9–11] of the excitations and finite size effects [12, 13] have been studied.

Apart from the basic DB also mobile breathers (MB), i.e. breathers that propagate through the system, have been found [14, 15]. As these breathers carry with them an additional internal degree of freedom they are from the very outset more complex objects, hinting a richer phenomenology than the 'simpler' solitary waves. However, much less is known about MBs than about immobile DBs. There is no proof of existence, yet strong numerical evidence that in certain systems these excitations are either stable or extremely long-lived [16, 17]. Mobile breathers have been found numerically both in Hamiltonian [18] and dissipative [19] systems. Conditions for MB existence are discussed e.g. in [20]. An interesting twist is given to the problem of the existence of propagating localised modes in [21], where, given the shape of such a mobile excitation, suitable equations of motion (more precisely on-site and/or interaction potentials) for a system supporting the excitation are constructed. Some further issues, like the question of the existence of a Peierls-Nabarro barrier for MBs or mobility of the localised excitation resulting from the instability of the localised mode against certain perturbations, are dealt with in e.g. [22, 23].

The system we will be looking at in this paper is the discrete sine-Gordon or standard Frenkel-Kontorova model. It describes a system of particles each of which is

[a] e-mail: matthias@unizar.es

subject to a periodic on-site potential and coupled harmonically to its nearest neighbours. In addition, we will consider the particles to be acted on by a periodic, external driving force and we also include dissipation. The equations of motion read

$$\frac{\mathrm{d}^2}{\mathrm{d}t^2}u_n = -\frac{1}{2\pi}\sin\big(2\pi u_n\big) + C\big(u_{n+1} + u_{n-1} - 2u_n\big) - \alpha\frac{\mathrm{d}}{\mathrm{d}t}u_n + F\sin(\omega_0 t). \quad (1)$$

The u_n denote the deviation of particle n from its corresponding minimum of the on-site potential. The system (1) supports mobile breather solutions as attractors of the dynamics, as was found numerically in [19]. Breather solutions can be obtained by continuation of solutions from the uncoupled limit ($C = 0$), where we have a system of uncoupled pendula. Due to the attractor property, the continuation is easier than for Hamiltonian systems. In the damped-driven chain, the coupling C is increased slightly, the system is allowed to relax, then C is again increased, and so on. In a Hamiltonian system, one usually has recourse to Newton methods [24].

In [19] two types of MBs have been found to exist in certain ranges of the coupling C: the so-called *induced fast breathers* and the *spontaneous slow breathers*. The former can be obtained by linearly perturbing a pinned breather with the velocity part of a certain localised eigenvector of the Floquet matrix. If the amplitude λ of this perturbation is larger than a critical value λ_c, the originally pinned breather starts to propagate along the chain. After a transient period, the velocity is independent of $\lambda > \lambda_c$. This last statement is at variance with what occurs for Hamiltonian systems [18]. The spontaneous slow breathers appear as stable solutions without requiring perturbations.

In Section 2 we look at the linearised equations of motion in order to obtain the phonon dispersion in the presence of damping. Simulations of breather-breather collisions are discussed in Section 3. One of the possible results of the interaction between the breathers during the collision is a two-breather bound state. The existence of such states in model (1) has already been reported in [19]. In Section 4 we present first systematic results on the properties of these special multibreather states, adding a discussion of some pertinent ideas in Section 5. Section 6 summarises our results and draws some conclusions. Interactions of colliding nonlinear localised excitations have been discussed by many authors. Closest to the work we present here is perhaps [25]. There the interaction of colliding breathers in a Hamiltonian sine-Gordon system very close to the continuum case has been studied. Our model contains dissipation and driving, the breather solutions are attracting configurations, and we are close to the anticontinuous (i.e. uncoupled, $C = 0$) limit; these differences obviously are pronounced. Further examples of the interaction of nonlinear localised modes upon collision in Hamiltonian lattices can be found for instance in [26] for the weakly perturbed Ablowitz-Ladik chain and in [27] for the DNLS equation. For the dissipative discrete sine-Gordon chain under a constant applied torque, bound states of kinks have been discussed in [28].

2 Phonons

Before discussing the interaction of breathers, in this section we look at phonons, i.e. solutions of the linearised equations of motion. The relevance to our problem is that the interaction between the (nonlinear) breathers is mediated by these phonons. The linearised equations of motion are

$$\frac{\mathrm{d}^2}{\mathrm{d}t^2}y_n = -\cos\big(2\pi u_n\big)y_n + C\big(y_{n+1} + y_{n-1} - 2y_n\big) - \alpha\frac{\mathrm{d}}{\mathrm{d}t}y_n, \quad (2)$$

obtained by replacing u_n with $u_n + y_n$ in (1) and keeping only terms of first order in y_n. Moreover, we wish to look specifically at parts of the chain far from the breather. There, the oscillations $u_n(t)$ of the breather solution are small, and (2) simplifies to

$$\frac{\mathrm{d}^2}{\mathrm{d}t^2}y_n = -y_n + C\big(y_{n+1} + y_{n-1} - 2y_n\big) - \alpha\frac{\mathrm{d}}{\mathrm{d}t}y_n. \quad (3)$$

We now consider the case that the site n_0 is executing the motion $y_{n_0}(t) = \exp(-i\omega t)$ and make the ansatz

$$y_n(t) = \exp[(-\xi + iq)|n - n_0| - i\omega t]. \quad (4)$$

Here ξ, q are real, ξ representing an inverse decay length and q a wavevector. Inserting (4) into (3), separating real and imaginary parts, we arrive at [19, 28]:

$$1 + \frac{1}{2C}\left(1 - \omega^2\right) = \cosh\xi\cos q, \quad \frac{\alpha\omega}{2C} = \sinh\xi\sin q. \quad (5)$$

These equations can be solved exactly for the dispersion relation under the influence of damping,

$$\omega^2 = 1 + 2C\left[1 - \cos(q)\sqrt{1 + \frac{\alpha^2(2C+1)}{4C^2[\sin(q)]^2} + \frac{\alpha^4[\cos(q)]^2}{16C^2[\sin(q)]^4}}\right] + \frac{\alpha^2}{2}[\cot(q)]^2. \quad (6)$$

From (5) we obtain straightforwardly

$$\xi = \operatorname{arcsinh}\frac{\alpha\omega}{2C\sin q}. \quad (7)$$

For a related result see [29]. Immediately we see from (6) that in the case $\alpha = 0$ we recover the dispersion relation for the undamped case. For α not too large, the relation (6) looks very much like the undamped dispersion relation. Only close to $q = 0$ and $q = \pm\pi$ are there pronounced differences, as $\omega(q) \to 0, \infty$ as $q \to 0, \pm\pi$, respectively, whereas in the undamped case $\omega(0) = 1$ and $\omega(\pm\pi) = \sqrt{1 + 4C}$. However, as can be derived from (7), frequencies outside the ω-region forming the phonon band

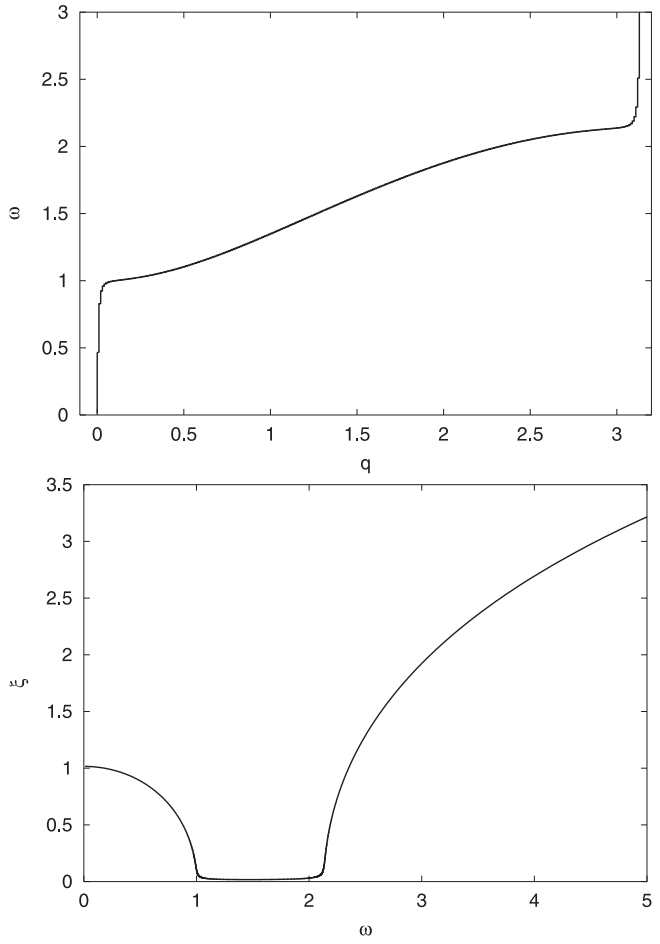

Fig. 1. Dispersion relation $\omega(q)$ (top) and inverse decay length $\xi(\omega)$ (bottom) for damping $\alpha = 0.02$ and coupling $C = 0.890$. Note that there is a 'window' of low damping, which is the analogue to the phonon band of the undamped case.

in the undamped case are subject to strong spatial damping, see Figure 1.

For later use let us recall that in the case of a moving source of phonon radiation, the frequencies and wavevectors are Doppler-shifted according to the equation

$$\omega(q) = \omega_s + v_s q. \tag{8}$$

Here ω and q are frequency and wavevector in the reference frame of the chain, ω_s is the emission frequency in the restframe of the source and v_s is the velocity of the source with respect to the chain. If on the other hand, there is a wave of frequency ω and wavevector q propagating in the chain, and we have a receiver moving at velocity v_r with respect to the chain, then the received frequency ω_r is

$$\omega_r = \omega - v_r q. \tag{9}$$

If both a moving source and a moving receiver are involved, the received frequency is obtained as

$$\omega_r = \omega_s + q(v_s - v_r). \tag{10}$$

Again, q is the wavevector in the chain. In the case $v_s = v_r$ the received frequency is the same as the emitted one. Note that equation (8) has to be solved numerically for q and ω in the case of complicated dispersion relations like (6).

3 Interaction of breathers

Two breathers approaching each other first feel the presence of the respective other one through the phonons emitted by this other breather. Though small in amplitude, if compared with the breather cores, these oscillations can affect the dynamics drastically. We have studied the collision of two 'spontaneous slow' breathers on a ring of $N = 1000$ particles, for system parameters $\alpha = 0.02, F = 0.02, \omega_0 = 0.2\pi, C = 0.890$ and a variety of initial conditions. The 2-breather initial conditions were constructed as follows: We started with one breather, located at a site l_0 (here 'located' means that the maximum elongation occurs at the site l_0), obtained from the continuation procedure described above. Then the configuration was allowed to evolve in time, for 1, 2, 3, and so on periods of the driving force, in our case up to 110 periods. The time evolution of the breather is quasiperiodic, thus after a period of the driving force the configuration is *not* the same as before up to a shift in position. The evolved breather configuration is then subject to a discrete translation, bringing the site of maximum elongation back to site l_0. Next, a new, 'inverted' configuration $u_n^{inv} = u_{N+1-n}, \frac{\mathrm{d}}{\mathrm{d}t}u_n^{inv} = \frac{\mathrm{d}}{\mathrm{d}t}u_{N+1-n}$ is created; the site of maximum elongation in the inverted configuration is $N + 1 - l_0$. We can now join the halves that contain the breathers of the inverted and the original (before the time evolution) configurations, obtaining a 2-breather initial condition. The discreteness and the driving force limit our choice of initial conditions. Both breathers have to be in dynamical states corresponding to the phase of the driving force, thus allowing only time shifts of integer periods of the driving between the breathers. Furthermore, the configurations have to be adjusted to the lattice, so only position shifts of integer multiples of the lattice constant are possible. In constructing the 2-breather configuration it is important to allow for a large initial separation between the breathers, in order to justify referring to them as individual excitations. In our case $l_0 = 800$, so the initial separation was 599, considering that part of the system along which the breathers were approaching each other, and 401 along the other part. As up to now we have determined the location of the breather by the site of maximum elongation, these values can hardly be more precise than one or two lattice constants. In the following we are using an improved definition of the position. We calculate the local energies

$$e_n = \frac{1}{(2\pi)^2}[1 - \cos(2\pi u_n)] + \frac{1}{2}\left(\frac{\mathrm{d}u_n}{\mathrm{d}t}\right)^2 \tag{11}$$

and *define* the position

$$X := \frac{\sum_{n=-2}^{n=2}(m+n)e_{m+n}}{\sum_{n=-2}^{n=2} e_{m+n}} \tag{12}$$

where the site m is determined as follows: We first look for sites where the distribution of the e_n has a local maximum above a certain threshold. The threshold serves to exclude local maxima in the e_n-distribution that are of phononic origin; the data shown in this paper have been obtained with a threshold of 0.01. If there occurs no other local maximum above the threshold within two sites to the left and right, then m is the site where the maximum occurs. This seems to happen in the majority of the cases. However, sometimes the distribution of the e_n can be 'M'-shaped, i.e. we have a sequence local maximum – local minimum – local maximum on three adjacent sites. In this case m is the site of the local minimum between the two local maxima of the 'M'. This definition of the position has the advantage that on the one hand it does not restrict to integer values the position X of the breather, contrary to what occurs when considering the site of maximum elongation as position of the breather. On the other hand it is local enough to only involve the breather, and not also extended phonon tails or perhaps already parts of a second breather in the system.

A configuration of two colliding breathers basically can evolve into 4 different types of final state: the breathers can rebounce, one of the breathers can be destroyed, both breathers can be destroyed, or the breathers can form a bound state. Figure 2 shows examples of these possibilities. We found that the scattering process is very sensitive to perturbations. Gaussian white noise acting on the system as an additional random force can change the *qualitative* outcome of a scattering process, though the noise is so weak that no thermal fluctuations are visible in the distribution of the e_n on a scale set by the peaks at the breather cores. For identical initial configurations we have observed reflection of the breathers, destruction and the formation of a bound state for different realisations of the noise.

Even without noise there are phonons in the system, those emitted by the breathers. These phonons mediate the direct breather-breather interaction, but they can also affect the scattering process indirectly, after travelling round the system (if we consider a ring) once or after being reflected from the boundaries (if we consider free boundary conditions). These phonons will be of small amplitude, nonetheless they can change the result of a collision qualitatively, i.e. they can for instance cause reflection instead of the formation of a bound state. The effect of these phonons can be observed if we change the boundary conditions from periodic to free or if the size of the system is increased. This sensitivity makes it very difficult to study the scattering process itself, the reliability of any approximation method being questionable. The bound states obtained from collisions turn out to be more robust than the process of their formation and are the subject of the next section. Before we turn to them, we would like to mention that such a sensitive dependence of the final state of a scattering process on the initial conditions has been reported in various publications, for instance [25, 30–32], which deal with the Hamiltonian continuum- or quasi-continuum case, and also in [26, 27], where lattices

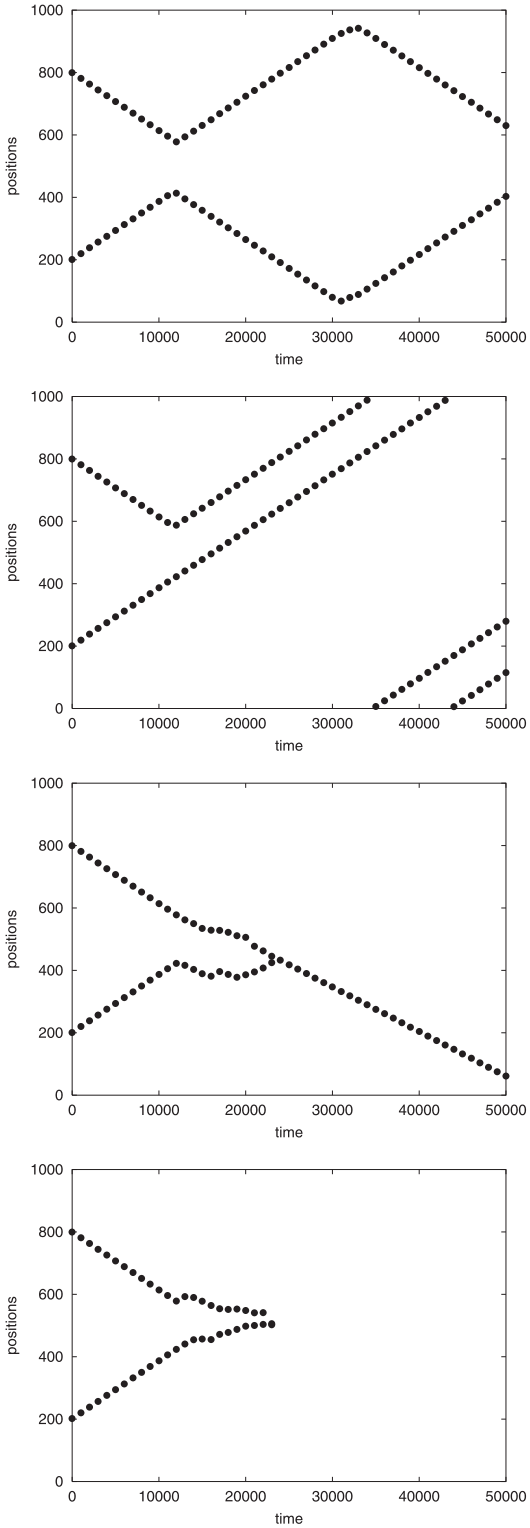

Fig. 2. Scattering processes with different final states, from top to bottom: reflection, bound state, destruction of one breather, destruction of both breathers. The positions of the colliding breathers were calculated according to (12). Note that the system forms a ring, therefore the bound state leaves the frame at the top edge and enters again at the bottom edge. In the case of reflection, the breathers reflect a second time when they approach each other again on the side of the ring opposite to the site of the first reflection.

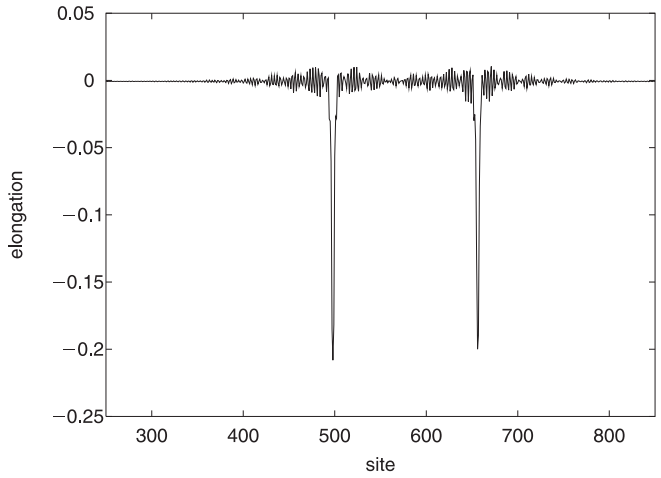

Fig. 3. A snapshot of a bound state configuration. The elongation of the particles from the equilibrium position as a function of the lattice site is plotted.

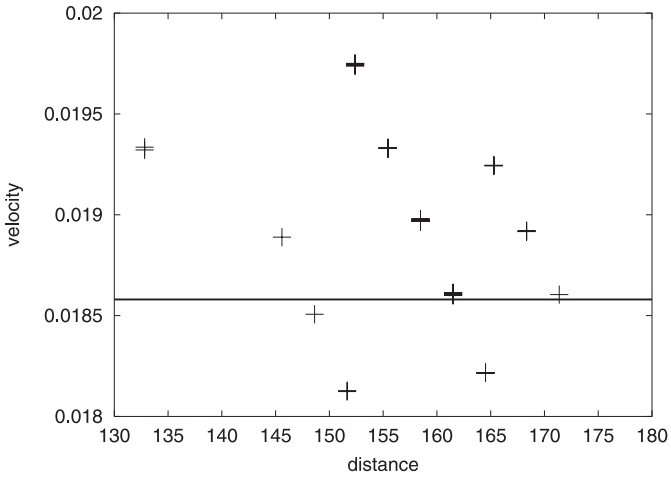

Fig. 4. Distance-velocity chart for 56 bound states obtained in numerical scattering experiments on a ring of 1000 particles for $\alpha = 0.02, F = 0.02, \omega_0 = 0.2\pi$ and $C = 0.890$. The straight line indicates the corresponding velocity of a single breather.

are addressed. We should stress, however, that due to the fundamental differences between autonomous Hamiltonian systems and the dissipative driven system we study, the nature of the possible final states is different. In our case, all the possible final states are attractors of the system, and the sensitivity is in the selection of the attracting final state given certain initial conditions and/or perturbations. In the Hamiltonian cases mentioned, apart from qualitatively different final states like reflection or merging of two colliding excitations, there can also occur sensitive but continuous variations of for instance the velocities of the final state excitations.

4 Bound states

From the scattering processes for the 110 initial conditions constructed as described in the previous section we obtained 56 bound states; this number includes those bound states that were formed in a collision of two breathers subsequent to one or several previous reflections of these breathers. A bound state is a configuration of two breather cores which are located at a certain distance from each other, the region between them containing phonon radiation. Also, bound states have tails, i.e. decaying phonon radiation in front of and behind the pair of breather cores. An example is shown in Figure 3. This structure propagates through the chain at a certain velocity v. The breather cores in a bound state continue to oscillate and usually do so out of phase with each other. Distance and velocity are not strictly constant as functions of time. They oscillate around a mean value and the details of these oscillations depend on the precise definition of these quantities. Generally, the distance d was calculated as $d(t) = |X_2(t) - X_1(t)|$, where X_1, X_2 are the positions of the two breathers as obtained from (12). The velocity v of the bound state is $v(t) = (v_1(t) + v_2(t))/2$, with $v_i(t) = (X_i(t) - X_i(t - \Delta t))/\Delta t, i = 1, 2$. Another possibility to define the velocities of the individual breathers for instance would be to take the time derivative of the definition of the position (12) and calculate the velocity from the configuration and velocities of the particles constituting the chain. The differences between the various definitions of course show that the breather is not a 'solid' object propagating through the chain and interacting with other excitations therein. This separation between the breather and the other modes is only an approximation, though a useful one. It, however, cannot grasp all the details of the motion of the breather, in particular because it is not possible to separate in a *unique* way the part of a configuration of the system which is due to the presence of a breather and the part which is due to other modes. Thus there is here some arbitrariness, because of which we will be restricting ourselves to time averages of distance and velocity.

In Figure 4 values of distance and velocity for the bound states we have obtained in the numerical scattering experiments are shown. The data points are grouped into three lines of negative slope, with the exception of the lowest distance value occuring. There are preferred values of the distance, and within one group these values are approximately equidistant. Also, a relation between distance and velocity is evident. We note, furthermore, that at fixed values of the model parameters (α, C, F, ω_0) several values are possible for the bound state velocity, but only one value is easily accessible for the single-breather velocity. The values shown in Figure 4 have been obtained as averages over 50,000 time units, where the positions of the breathers have been calculated from the configurations every time unit, and in turn from them the values of distance and velocity. The data shown in the figure are for the 56 bound states found from 110 initial conditions, without us having a possibility to predict whether a given initial condition leads to a bound state and if so, what

its distance-velocity pair will be. Consequently, we do not know whether the points in Figure 4 represent *all* possible bound states or whether more bound states would show up in runs over for instance 10,000 initial conditions. A reasonable guess is that the bound states we have found are those appearing with the highest probabilities, i.e. those with the largest basins of attraction.

The interaction between the breathers is mediated by phonons and thus the features appearing in Figure 4 will be connected with properties of the linear, extended excitations. Therefore, we study the spectra of the oscillations between the breather cores. We select one site on the ring and record the oscillations of the corresponding particle as it is passed by the bound state. Then, the time interval of the oscillation caused by the phonons in the region between the breather cores is subject to a Fast Fourier Transform (FFT). The lines of the spectra are the basic driving frequency ω_0, present everywhere in the chain, and phonons the frequencies of which are obtained by Doppler-shifting with velocity v frequencies $3\omega_0 + 2\pi vn$, n integer. The frequency $2\pi v$ arises because the propagation of the configuration along the chain amounts to a perturbation of frequency $2\pi v$ (the lattice constant is 1). The frequencies to be shifted are combination frequencies of the third harmonic of the driving force with this frequency. As for the Doppler-shifts, which also occur because of the translatory motion of the bound state, we have to take into account the following: Since we are looking at the region between the breather cores, one of the cores emits the phonons in question in the direction of the motion, the other in the opposite direction. So one given frequency turns into two, because it is shifted both to a higher and a lower value. The Doppler-shifted frequencies can easily be calculated numerically. In Figure 5 the calculated values are compared with the spectra determined by FFT. As we can see, the phonon frequencies are well reproduced by the values obtained from the Doppler effect. Note that some minor lines do not stem from shifts of $3\omega_0+2\pi vn$ but from shifts of $\omega_0+2\pi vn$. Due to the ω-dependence of the inverse decay length ξ (see Fig. 1), frequencies in the vicinity of $3\omega_0 = 0.6\pi \approx 1.885$ can propagate under comparatively weak damping, i.e. ξ is small and thus their decay length is large. Frequencies close to ω_0, on the other hand, are subject to much stronger damping. The phonon frequency a breather receives is equal to the emitted one, according to equation (10), as the two breathers in a bound state fulfil $v_s = v_r = v$.

The phonons incident on a breather exert an additional force on the breather, which, as our numerical results show, can change its velocity. If, for a pair of breathers, these changes are such that the resulting velocities are equal, we observe the formation of a bound state. The necessity of the mutual influence of the breathers is clearly shown by the following observation from simulations: If one half of a bound state is replaced with a homogeneous configuration, leaving only one breather core in the system, this configuration evolves to a single breather. Its velocity is equal to the value indicated in Figure 4 for a single breather, i.e. the changes in the velocity cannot

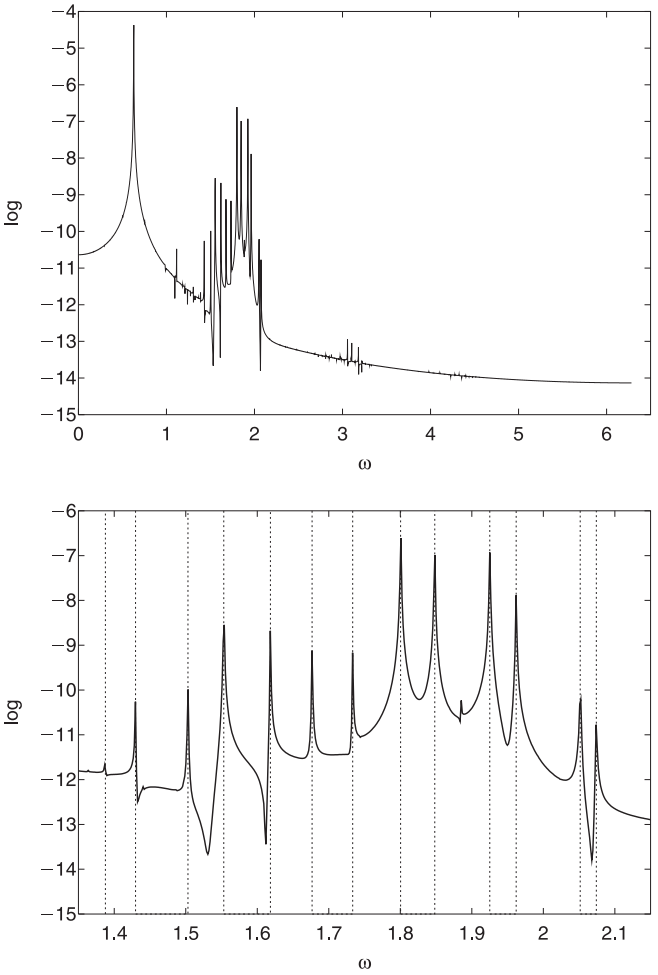

Fig. 5. Spectrum of the particle oscillations for one of the bound states (see text). Logarithm of the FFT output as a function of ω. The bottom panel is a zoom of the top one. The straight lines in the lower panel indicate the ω-values in the predicted spectrum (Doppler shifts of $3\omega_0 + 2\pi vn$). The spectra of the other bound states have an analogous structure.

persist without the second breather. Thus a bound state can be interpreted as a pair of single breathers under an additional force created by the respective partner of each breather.

We have performed a continuation of a bound state with respect to the coupling C. Results are shown in Figure 6. We first look at the distance. In the first series of the continuation we started at $C = 0.89$ on the lower of the two branches shown and continued both to higher and lower values of the coupling in steps of 0.001 and a relaxation period of 5000 time units after each step. At $C = 0.894$ the system jumped to the upper branch, which seems to be more stable in this parameter regime. We obtained the part $C > 0.894$ of the lower branch by a more careful simulation, using relaxation times of 5000 time units and C-steps of 0.0001. Despite this, it became increasingly difficult to follow the lower branch to higher values of the coupling, therefore we stopped. The part

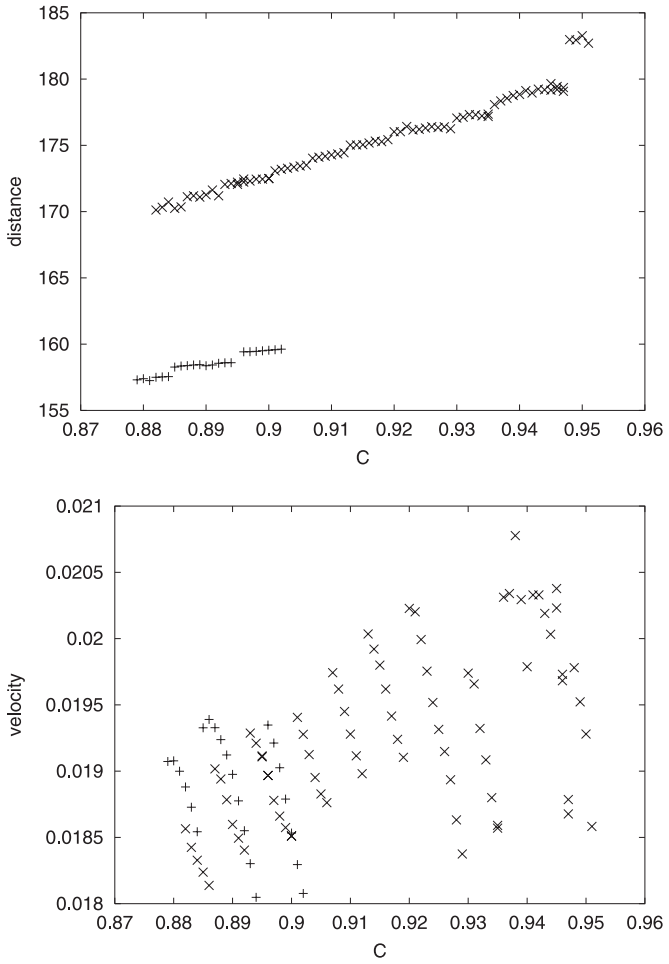

Fig. 6. Results of the continuation of a bound state with respect to the coupling C. The other parameters have been $\alpha = 0.02, F = 0.02, \omega = 0.2\pi$. Top: The distance as a function of C. Bottom: The velocity as a function of C. (+) refers to the lower, (×) to the upper branch of the top panel.

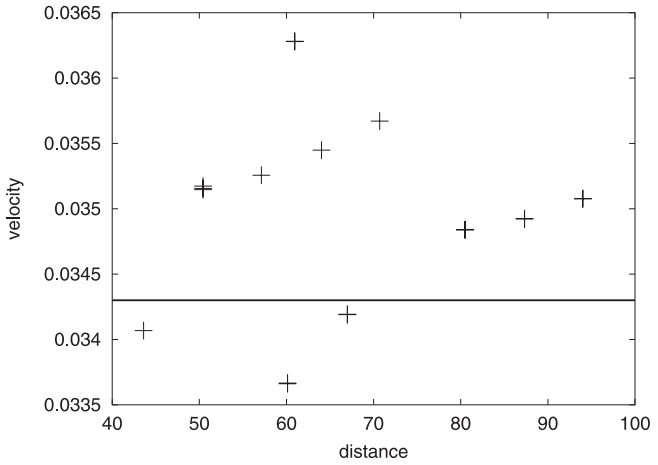

Fig. 7. Distance-velocity chart like Figure 4 (also same parameters) however for 19 bound states in a velocity range around the velocity of an induced fast breather. The latter value is indicated by the straight line.

of the upper branch below $C = 0.894$ was obtained by continuing downwards from $C = 0.896$. The existence of several branches (many more than just two) can be expected, because one branch corresponds to only one of many bound states at a fixed value of C, see Figure 4. For both branches the bound state became unstable after a number of C-steps. This indicates that despite the relaxation time of 5000 time units, the configurations accumulated perturbations, which at a certain level destroyed the bound state. In this case the last stable configuration was allowed to evolve in time over 50,000 time units at its corresponding value of C and we then used the resulting configuration as initial one for further continuation.

The discreteness of the system (lattice constant 1) is reflected in the tiny steps occuring whenever the distance has increased by 1. The same 'periodicity' shows up in the velocities. We observe a jump when the distance jumps, followed by a gradual change in the velocity, in most cases a decrease when C increases.

For large C-values the observed patterns in the distance and the velocity graphs become irregular. This indicates a reduction of bound state stability as the coupling approaches the value $C_{pin} \approx 0.96$ above which single breathers were found to be pinned [19]. Likewise, the continuation to lower values of C terminates near $C = 0.879$, the value below which single spontaneous slow breathers have not been found, and where, according to our numerical results, the bound state becomes unstable.

Ending this section we want to mention that we also have found bound states of breathers in a velocity range around the velocity of an induced fast breather, see Figure 7. We obtained one such bound state as a result of noise acting on a 'slow' bound state. The other bound states were obtained by manipulating this bound state configuration, for instance by replacing the part of the configuration between the cores with a homogeneous one.

5 A conjecture on ILM binding

As stated in Section 3, not every collision of two breathers leads to a bound state. Furthermore, Figure 4 shows that the values of distance and velocity are not arbitrary. In this section we want to discuss some ideas connected with these observations. We have already pointed out above that the interaction between the ILMs is mediated by phonons, which can effect a change of the ILM velocity. It is natural to expect that the size and sign of this change will depend on the phonon parameters, i.e. frequency, phase (relative to the ILM oscillations) and amplitude. Figure 5 shows that there are many phonon frequencies that can play a role. For the interaction process in general, none of these frequencies can in principle be ruled out, in particular if we take into account the sensitivity of the scattering to perturbations. However, if we consider bound states, the following conclusions are plausible: In the rest frame of

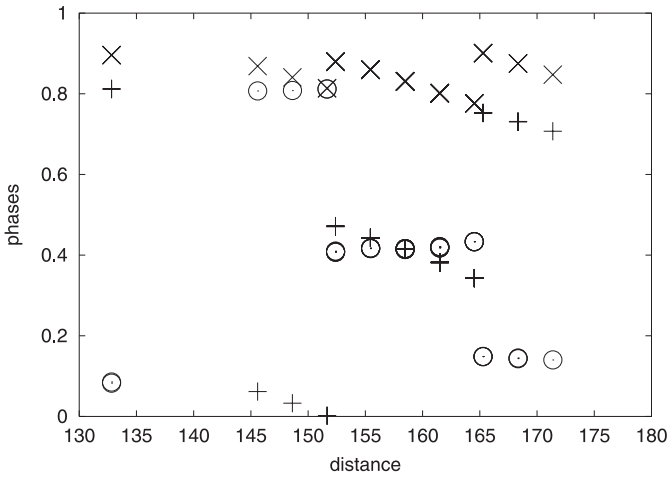

Fig. 8. The phases in units of 2π for the bound states of Figure 4. $(+) : \delta_1$, $(\times) : \delta_2$, $(\circ) : \delta_2 - \delta_1$.

the bound state, the dominating contribution to the ILM dynamics is periodic with a frequency spectrum consisting of ω_0 and its higher harmonics; the additional frequencies arising from the motion of the lattice through the bound state are perturbations. The bound state is an attracting steady state configuration of the system and this suggests that the phonon frequencies involved in the binding share the periodicity of the bound ILMs (rather than connecting the binding to phonons the frequencies of which are incommensurate with the ILM oscillation). This leaves us with ω_0 and its higher harmonics. From the behaviour of the inverse decay length ξ (see Fig. 1) it is evident that only phonons with frequencies close to $3\omega_0$ can propagate over larger distances. Therefore we conjecture that phonons with frequencies (in the restframe of the lattice) which are Doppler-shifts of $3\omega_0$ are mainly responsible for ILM binding.

From the bound states we have obtained we can evaluate the corresponding phonon phases. In order to do so, let us introduce some quantities. Out of the frequency $3\omega_0$ by Doppler-shift we obtain two frequencies, $\omega_1 > 3\omega_0 > \omega_2$, with corresponding wavevectors $q_1 > q_2$ and wavelengths $\lambda_1 < \lambda_2$. With d the distance between the breather cores, we can write

$$q_1 d = 2\pi m + \delta_1, \quad q_2 d = 2\pi n + \delta_2 \quad (0 \leq \delta_{1,2} < 2\pi) \quad (13)$$

where m, n are integers, and $\delta_{1,2}$ the phase shifts necessary for a stable bound state. Combining the two equations we find

$$d = \frac{2\pi(m-n)}{q_1 - q_2} + \frac{\delta_1 - \delta_2}{q_1 - q_2} = \lambda \left(m - n - \frac{\delta_2 - \delta_1}{2\pi} \right) \quad (14)$$

with $\lambda = 2\pi/(q_1 - q_2)$. The values for the phases we have obtained for the bound states of Figure 4 are shown in Figure 8. Furthermore it turns out that $m - n$ is constant within one group in Figure 4, in fact it is constant, $m - n = 5$, for all bound states in the figure except for the lowest distance shown, where $m - n = 4$. Within one group the phase difference $\delta_2 - \delta_1$ is also constant, see Figure 8. The changes in the distance within one group thus are entirely due to changes in λ. If the velocity decreases, so does $q_1 - q_2$, and therefore λ and in turn also the distance d increase.

The results clearly confirm our expectation about the phases, as Figure 8 gives the phase pertinent to each distance-velocity pair. Arbitrary values of the phases $\delta_1,\ \delta_2$ on the other hand would, according to (13) and (14), evidently lead to arbitrary distance-velocity combinations, in contradiction to our numerical results.

Besides the fact that it is trivial, the expectation on the amplitude is also evident. First from Figure 2, where we see that during the initial part the excitations propagate apparently without disturbing each other. Second from the fact that according to equation (14) at fixed $q_1,\ q_2,\ \delta_1$ and δ_2 changes to the integer quantity $m - n$ should give a family of bound states the members of which share the same velocity but differ in the distance. Due to the non-vanishing decay length ξ, varying distances between ILMs in a bound state result in varying amplitudes of the incident binding-mediating phonons. The results show that for the bound states we have studied, only two values for $m - n$ appear, namely 5 and 4, the former moreover being strongly preferred.

We have similarly analysed the bound states obtained in the C-continuation, Figure 6; the results are shown in Figure 9. For the lower branch, from equations (13), we have $(m, n) = (53, 48)$, for the upper branch $(m, n) = (57, 52)$, and $(m, n) = (58, 53)$ for $C > 0.947$. It will be observed that here also $m - n = 5$ in all cases.

6 Summary

In this article we have presented phenomenological results on breather bound states. These special multibreather states can be created in breather-breather collisions and turn out to be attractors of the system. Two major characteristics of such a bound state are the distance between the two breather cores and the propagation velocity of the bound state. According to data obtained from simulations of the lattice dynamics, these two quantities are clearly related. We have interpreted a bound state as a pair of single breathers, where each breather, in addition to the spatially homogeneous external driving force, also is subject to a force originating from the phonons emitted by the other breather in the pair. This additional force changes the velocity of the breather. We have conjectured that the binding between the ILMs in the bound state is effected by the phonons that are the Doppler-shifted radiation emitted by the third harmonic of the ILM oscillation. Based on this conjecture we have analysed the phase relation between these phonons and the ILM oscillation and found that for given bound state characteristics (distance and velocity) a particular value of this phase is necessary in order to have a bound state. The relevance of the phonon amplitude in this context has also been confirmed.

An important observation is that for a given set of values of the model parameters (coupling, damping,

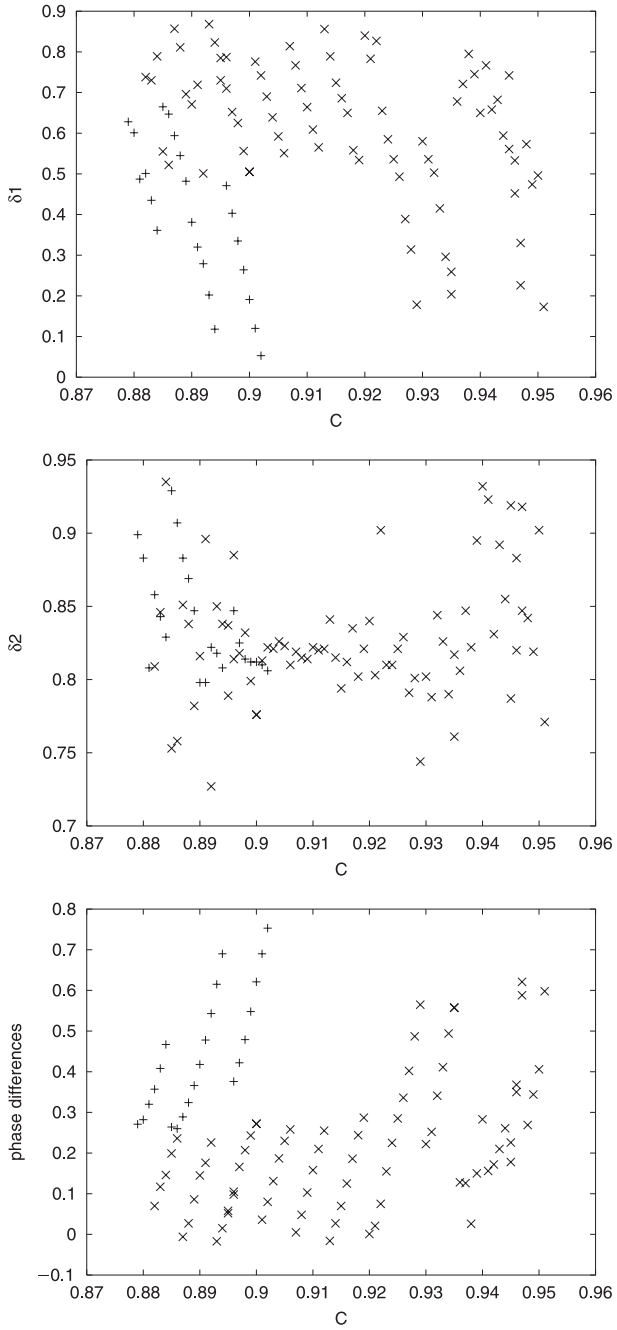

Fig. 9. The phases for the continuation in the coupling: δ_1 (top) and δ_2 (middle). The phase differences $\delta_2 - \delta_1$ are shown in the bottom panel. Again, (+) refers to the lower and (×) to the upper of the two branches shown in Figure 6 (top).

amplitude and frequency of the driving) there are several easily accessible values of the velocity of a bound state, but usually only one value of the velocity of a single breather. This indicates that the formation of breather bound states can have important implications for the transport properties of the system.

MM acknowledges a fellowship from the European Commission within the Research Training Network (RTN) LOCNET, contract HPRN-CT-1999-00163. LMF acknowledges an EU senior Marie Curie fellowship HPMF-CT-2002-01965 and ITE (FORTH) at Heraklion for the kind hospitality during the completion of this work. Support from project BFM2002-00113 is also acknowledged. The authors thank P.J. Martínez and Fernando Falo for discussions.

References

1. A.R. Bishop, J.A. Krumhansl, S.E. Trullinger, Physica D **1**, 1 (1980)
2. R. Camassa, J.M. Hyman, B.P. Luce, Physica D **123**, 1 (1998)
3. A.J. Sievers, S. Takeno, Phys. Rev. Lett. **61**, 970 (1988)
4. S. Takeno, A.J. Sievers, Solid State Commun. **67**, 1023 (1988)
5. S. Takeno, K. Kisoda, A.J. Sievers, Prog. Theor. Phys. Suppl. **94**, 242 (1988)
6. R.S. MacKay, S. Aubry, Nonlinearity **7**, 1623 (1994)
7. S. Aubry, Physica D **103**, 201 (1997)
8. J.-A. Sepulchre, R.S. MacKay, Nonlinearity **10**, 679 (1997)
9. D. Bambusi, Nonlinearity **9**, 433 (1996)
10. R.S. MacKay, J.-A. Sepulchre, Physica D **119**, 148 (1998)
11. J.L. Marín, S. Aubry, L.M. Floría, Physica D **113**, 283 (1998)
12. J.L. Marín, S. Aubry, Physica D **119**, 163 (1998)
13. A.M. Morgante et al., J. Phys. A: Math. Gen. **35**, 4999 (2002)
14. S. Takeno, K. Hori, J. Phys. Soc. Jpn **59**, 3037 (1990)
15. S. Takeno, K. Hori, J. Phys. Soc. Jpn **60**, 947 (1991)
16. K. Hori, S. Takeno, J. Phys. Soc. Jpn **61**, 2186 (1992)
17. K. Hori, S. Takeno, J. Phys. Soc. Jpn **61**, 4263 (1992)
18. D. Chen, S. Aubry, G.P. Tsironis, Phys. Rev. Lett. **77**, 4776 (1996)
19. J.L. Marín et al., Phys. Rev. E **63**, 066603 (2001)
20. S. Flach, K. Kladko, Physica D **127**, 61 (1999)
21. S. Flach, Y. Zolotaryuk, K. Kladko, Phys. Rev. E **59**, 6105 (1999)
22. S. Aubry, T. Cretegny, Physica D **119**, 34 (1998)
23. S. Flach, C.R. Willis, Phys. Rev. Lett. **72**, 1777 (1994)
24. J.L. Marín, S. Aubry, Nonlinearity **9**, 1501 (1996)
25. S.V. Dmitriev, Yu.S. Kivshar, T. Shigenari, Phys. Rev. E **64**, 056613 (2001)
26. S.V. Dmitriev et al., Phys. Rev. E **68**, 056603 (2003)
27. I.E. Papacharalampous et al., Phys. Rev. E **68**, 046604 (2003)
28. A.V. Ustinov, B.A. Malomed, S. Sakai, Phys. Rev. B **57**, 11691 (1998)
29. S. Flach, M. Spicci, J. Phys. Cond. Mat. **11**, 321 (1999)
30. M. Peyrard, D.K. Campbell, Physica D **9**, 33 (1983)
31. K.A. Gorshkov, A.S. Lomov, M.I. Rabinovich, Nonlinearity **5**, 1343 (1992)
32. J. Yang, Y. Tan, Phys. Rev. Lett. **85**, 3624 (2000)